

Rethinking Thorne–Żytkow Object Formation: The Fate of X-ray Binary LMC X-4 and Implications for Ultra-long Gamma-ray Bursts

TENLEY HUTCHINSON-SMITH ^{1,2}, ROSA WALLACE EVERSON ^{1,2,*}, ALDO BATTA ^{3,4,2}, RICARDO YARZA ^{1,5,†},
ANGELA A. TWUM ¹, JAMIE A.P. LAW-SMITH ^{6,7} AND ENRICO RAMIREZ-RUIZ ^{1,2}

¹*Department of Astronomy and Astrophysics, University of California, Santa Cruz, CA 95064, USA*

²*Niels Bohr Institute, University of Copenhagen, Blegdamsvej 17, 2100 Copenhagen, Denmark*

³*Instituto Nacional de Astrofísica, Óptica y Electrónica. Tonantzintla, Puebla 72840, México*

⁴*Consejo Nacional de Humanidades Ciencias y Tecnología, Av. Insurgentes Sur 1582, 03940, Mexico City, México.*

⁵*Texas Advanced Computing Center, University of Texas, Austin, TX 78759, USA*

⁶*Department of Astronomy and Astrophysics, University of Chicago, Chicago, IL, 60637, USA*

⁷*Kavli Institute for Cosmological Physics, University of Chicago, Chicago, IL, 60637, USA*

ABSTRACT

We present a start-to-end simulation aimed at studying the long-term fate of high mass X-ray binaries and whether a Thorne–Żytkow object (TŻO) might ultimately be produced. We analyze results from a 3D hydrodynamical simulation that models the eventual fate of LMC X-4, a compact high mass X-ray binary system, after the primary fills its Roche lobe and engulfs the neutron star companion. We discuss the outcome of this engulfment within the standard paradigm of TŻO formation. The post-merger angular momentum content of the stellar core is a key ingredient, as even a small amount of rotation can break spherical symmetry and produce a centrifugally supported accretion disk. Our findings suggest the inspiraling neutron star, upon merging with the core, can accrete efficiently via a disk at high rates ($\approx 10^{-2} M_{\odot}/s$), subsequently collapsing into a black hole and triggering a bright transient with a luminosity and duration typical of an ultra-long gamma-ray burst. We propose that the canonical framework for TŻO formation via common envelope needs to be revised, as the significant post-merger accretion feedback will unavoidably unbind the vast majority of the surrounding envelope.

Keywords: binaries: close — stars: evolution — stars: interiors

1. INTRODUCTION

High mass X-ray binaries (HMXBs) are X-ray emitting sources commonly featuring an early-type massive star and an accreting neutron star (see, e.g., Liu et al. 2006; Falanga et al. 2015). A critical juncture in the life of a HMXB is the period just after the primary fills its Roche lobe and engulfs the neutron star companion (Paczynski 1976; van den Heuvel 1976). Mass transfer is unstable and a catastrophic merger with the stellar core cannot be avoided (see, e.g., Belczynski et al. 2002; Qin et al. 2019; Gallegos-Garcia et al. 2022; Lotine et al. 2023). The further evolution of the merger product has been speculated to potentially give rise to a Thorne–Żytkow object (TŻO; Thorne & Żytkow 1975, 1977).

A TŻO is a conjectured type of star containing a neutron star at its core, claimed to be formed by the engulfment of a neutron star by an evolving stellar companion (Thorne & Żytkow 1975, 1977). While we are used to thinking about stars being solely energized by nuclear fusion, TŻOs are speculated to be powered by mass accretion onto the central compact object. Recently, a chemical anomaly in the red supergiant star HV 2112 in the Small Magellanic Cloud was speculated to be produced by an embedded accreting compact object (Levesque et al. 2014). The claim that HV 2112 might be a TŻO candidate arises from the anomalously high ratios of calcium, lithium, ruthenium, and molybdenum, which have been predicted to exist inside the exotic accretion-powered stellar interiors of TŻOs. While this claim has incurred numerous rebuttals (Tout et al. 2014; Maccarone & de Mink 2016; Beasor et al. 2018; O’Grady et al. 2020), it has reinvigorated the construction of numerical models of TŻOs (e.g., Farmer et al. 2023), particularly in the context of common envelope (CE) evolution.

While most TŻO calculations suppose a non-rotating, spherically symmetric structure (Thorne & Żytkow 1977;

Corresponding author: Tenley Hutchinson-Smith

tenley@ucsc.edu

* NSF Graduate Research Fellow

† NASA FINESST Fellow

Frontera Computational Science Fellow

arXiv:2311.06741v1 [astro-ph.HE] 12 Nov 2023

Biehle 1991; Cannon et al. 1992; Farmer et al. 2023), formation via CE will invariably lead to the NS being surrounded by stellar material with significant rotational support. Understanding the angular momentum content of the infalling gas is thus critical when thinking about the post-formation evolution of TZO. This is because the angular momentum content of the post-merger material determines if a disk will form: if there is no rotation, only Bondi-like accretion will ensue (Cannon et al. 1992), which, in turn, has important implications for how accretion will advance (Lee & Ramirez-Ruiz 2006; Murguía-Berthier et al. 2020; Halevi et al. 2023).

Motivated by this, we present here and in a companion paper by Everson et al. (2023) a study of the long-term fate of high mass X-ray binaries and whether a TZO might ultimately be produced. In this work, we use the binary system LMC X-4 in the neighboring Large Magellanic Cloud (LMC) satellite galaxy to guide our understanding of such outcomes: LMC X-4 is a highly compact, two-star system consisting of a pulsar and a massive stellar companion and currently has one of the most accurate determinations of the orbital parameters of high mass X-ray binaries available to date (Falanga et al. 2015). LMC X-4 thus appears to be an ideal progenitor candidate for a merged stellar remnant with an embedded neutron star in its core, offering clear constraints for the formation of TZOs. In a companion paper, Everson et al. (2023) expands this analysis by exploring the potential formation pathways of TZOs across a broad parameter space of field binaries comprised of an evolved star and stellar-mass compact object, as well as the expected outcomes for such systems.

This paper is structured as follows. In §2, we show using stellar evolution calculations that, as expected, the LMC X-4 binary system will merge via common envelope. Our stellar evolution models after the primary fills its Roche Lobe are used as initial conditions for three-dimensional (3D) hydrodynamical calculations, which are described in §3. Our results are then discussed in §4, with a summary of this work in §5.

2. FORWARD MODELING THE PRE-MERGER EVOLUTION OF LMC X-4

In order to explore the potential for TZO formation during the expected merger of the LMC X-4 system, we develop initial conditions based on the best current mass, size, and kinematic constraints available (Falanga et al. 2015), forward-evolve them with MESA to common envelope onset, then map the resulting future system into three dimensional hydrodynamics and evolve it through CE and merger.

2.1. Properties of LMC X-4

Over a decade of monitoring with multiple instruments (Liu et al. 2006; Falanga et al. 2015) has provided strong constraints on the properties of LMC X-4. According to Falanga et al. (2015), this HMXB system is comprised of a $1.57 \pm 0.11 M_{\odot}$ neutron star (NS) that is accreting from its $18 \pm 1 M_{\odot}$ stellar companion. The companion, hereafter referred to as the primary, somewhat underfills its Roche lobe

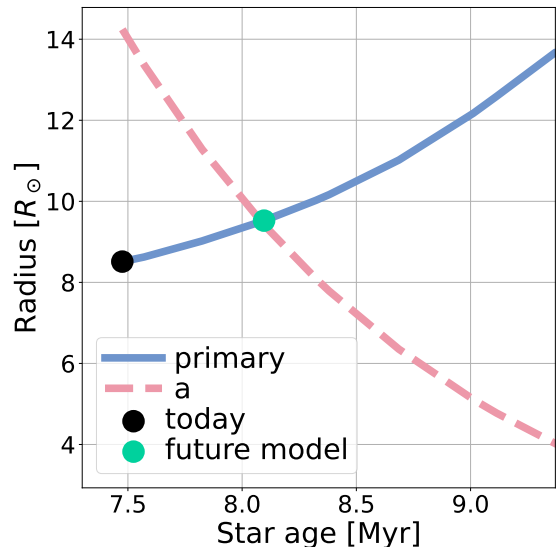


Figure 1. The predicted radial evolution of the primary star as calculated by MESA using the mean LMC metallicity of $[\text{Fe}/\text{H}]=-0.42$. The initial mass of the model is $18 M_{\odot}$, with mass loss $2.4 \times 10^{-7} M_{\odot} \text{ yr}^{-1}$ (Chernov 2020). The selected model (black symbol) is consistent with the properties given by Falanga et al. (2015) within 1σ . The model used for the hydrodynamical simulation performed with FLASH is marked with a turquoise symbol in the panel. At this stage, the donor has overfilled its Roche lobe and its radial scale matches the forward-evolved separation a (dashed line).

with a stellar radius of $7.4 \pm 0.4 R_{\odot}$. The system has a separation of $14.2 \pm 0.2 R_{\odot}$ and an observed orbital period of 1.408 days. Falanga et al. (2015) estimates the orbital period change \dot{P}/P as $-1.0 \times 10^{-6} \text{ yr}^{-1}$, suggesting a gradual tightening of the orbit. The estimated mass loss rate of the primary due to winds is $2.4 \times 10^{-7} M_{\odot} \text{ yr}^{-1}$ (Chernov 2020), which alone cannot account for the estimated \dot{P}/P value.

2.2. Stellar Models

We begin with modeling the evolution of the primary from the present time to the onset of CE using the MESA Isochrones and Stellar Tracks (MIST) package (Dotter 2016; Choi et al. 2016) with MESA v7503 (Paxton et al. 2011, 2013, 2015). The MIST framework is chosen due to its calibration to observations, including in the LMC. We evolve the primary as a single star using the mean LMC metallicity of $[\text{Fe}/\text{H}]=-0.42$ (Choudhury et al. 2021). We choose our initial mass range $[16,20] M_{\odot}$ to be consistent with the 2σ mass estimates from Falanga et al. (2015). This allows us to create a grid of potential models that will be narrowed down based on the properties of the primary star.

Because the evolution of the orbital period is not totally independent of the evolution of the primary, we consider both. Prior work has attempted to explain the \dot{P}/P value of LMC X-4 with conservative mass transfer (Safi-Harb & Ögelman 1996) and changes in the primary’s moment of in-

ertia (Levine et al. 2000). Upon revisiting these works, in the former case the mass transfer rate required is much higher than the observationally derived mass loss values for the primary, and in the latter case, the formalism cannot match the measured \dot{P}/P when applied to up-to-date stellar models in the appropriate stage of evolution (Chernov 2020). For this system, wind mass loss serves only to make orbital tightening more difficult.

Recent work by Chernov (2020), however, demonstrates that tides alone are sufficient to explain LMC X-4’s orbital tightening. Though the rate of orbital tightening does include effects from winds, mass transfer, and the primary’s change in moment of inertia, it’s not possible to completely distinguish these effects with those of the degree of corotation on dynamical tides. This leaves LMC X-4’s separation as a function of time $a(t)$ as our last additional constraint on the primary, as the Roche lobe acts as a size constraint and trigger of mass loss for our models. The models with initial masses of $18 M_{\odot}$ and $19 M_{\odot}$, with mass loss as prescribed by Chernov (2020), are consistent with the properties given by Falanga et al. (2015) within 1σ , and as the three dimensional hydrodynamical results for both are qualitatively similar, we present those from the $18 M_{\odot}$ model below.

Using the size of the primary’s Roche lobe, we allow the models to lose mass as they approach the end of the main sequence via winds and a radius-limited prescription for Roche lobe overflow. When the model reaches the observed mass and radius constraints (black symbol in Figure 1), we mark that model as “today,” then allow the star to continue its evolution while evolving the separation a using the observed \dot{P}/P . We then map the resulting “future” model, in which the donor has overflowed its Roche lobe and its radius equals the forward-evolved separation a (turquoise symbol in Figure 1), into 3D for the simulation of CE and merger.

3. STUDYING THE FATE OF X-RAY BINARY LMC X-4 WITH HYDRODYNAMICAL SIMULATIONS

3.1. FLASH Setup

We map the properties of the MESA profile (density, pressure, temperature, and composition) onto a three dimensional grid using FLASH version 4.32 (Fryxell et al. 2000). Our numerical scheme is adapted from Wu et al. (2020), which was originally developed by Guillochon et al. (2009) and Guillochon & Ramirez-Ruiz (2013), and subsequently upgraded by Law-Smith et al. (2019, 2020a,b). The upgraded version uses an extended Helmholtz equation of state (Timmes & Swesty 2000) to track individual elements as described in Law-Smith et al. (2019) and Wu et al. (2020). The reader is referred to these works for further numerical details. A brief summary including key aspects and alterations to the setup is given below.

To set up the initial model, we first relax the MESA profile in FLASH for a few dynamical timescales. The computational domain is cubic with volume $(60R_{\odot})^3$ and is comprised of an 8^3 block grid with a minimum cell size of $0.02 R_{\odot}$. During the relaxation process, a point mass, repre-

sented the NS with $M_{\text{ns}} = 1.57M_{\odot}$, is introduced at $9R_{\odot}$. The primary star has a radial scale $\approx 9.4R_{\odot}$ when it overfills its Roche lobe (Figure 1). The NS is initially at rest but its velocity is slowly augmented as the relaxation process ensues until reaching a circular Keplerian velocity. At the time the relaxation finishes, the model of the primary star is in hydrostatic equilibrium and the inspiral trajectory of the NS is calculated self-consistently (Wu et al. 2020). The properties of the merger remnant are found to be rather indifferent to the exact initial conditions of the NS’s velocity, as long as it is close to Keplerian. We stop the simulation once the NS sinks into the center of the primary’s core ($t = 13.8$ hr).

3.2. Dynamical Inspiral

Now we turn our attention to LMC X-4 at the onset of CE and beyond. As the engulfment proceeds (from left to right in the top three panels of Figure 2), the NS plunges dynamically into the stellar core of the mildly evolved primary star. This steep plunge-in is driven by strong drag forces, which are significantly higher than those predicted by Bondi–Hoyle–Lyttleton accretion theory (Hoyle & Lyttleton 1939) when the stellar density gradients are included, as shown by MacLeod & Ramirez-Ruiz (2015a,b), MacLeod et al. (2017a) and Everson et al. (2020). We compare the numerical trajectories with the modified drag predictions presented in MacLeod & Ramirez-Ruiz (2015b) and find rough agreement with the dynamical plunge seen in Figure 2.

As can be seen from Figure 2, the NS disturbs a non-negligible fraction of the outer stellar envelope during inspiral. It then crosses the core without disrupting it and settles inside the stellar core after about 13.8 hr. As a result of the merger, the NS injects energy and angular momentum (via spiral waves) into the primary and unbinds a small fraction of the envelope material. The bottom panels in Figure 2 show specific energy, $\varepsilon = \varepsilon_{\text{kin}} + \varepsilon_{\text{grav}}$ (the sum of specific kinetic and potential energy while the internal energy is not included). The coral region corresponds to unbound material ($\varepsilon > 0$) while the green region corresponds to bound material ($\varepsilon < 0$). At early times, $\varepsilon < 0$ for most cells in the box. At the final time depicted in Figure 2, a non-negligible fraction (see Section 3.3 for details) of the material in the box (except for the surviving core) has $\varepsilon > 0$. In what follows we engage in a more comprehensive evaluation of the ejection of material during the merger.

3.3. Mass Ejection during Merger

Figure 3 shows, as a function of the mass coordinate, the binding energy of the envelope and the change in the orbital energy from the start of the inspiral, using the properties of the stellar model that we have selected as the initial condition for the hydrodynamical simulation. This shows the necessary conditions for effective envelope ejection, which are expected to be satisfied when the change in orbital energy of the NS, lost through drag during inspiral, is similar to the envelope’s binding energy at a particular mass coordinate, known as the $\alpha = (E_{\text{grav}}/\Delta E_{\text{orb}}) = 1$ condition. The calculations presented in Figure 3 predict that the NS would unbind

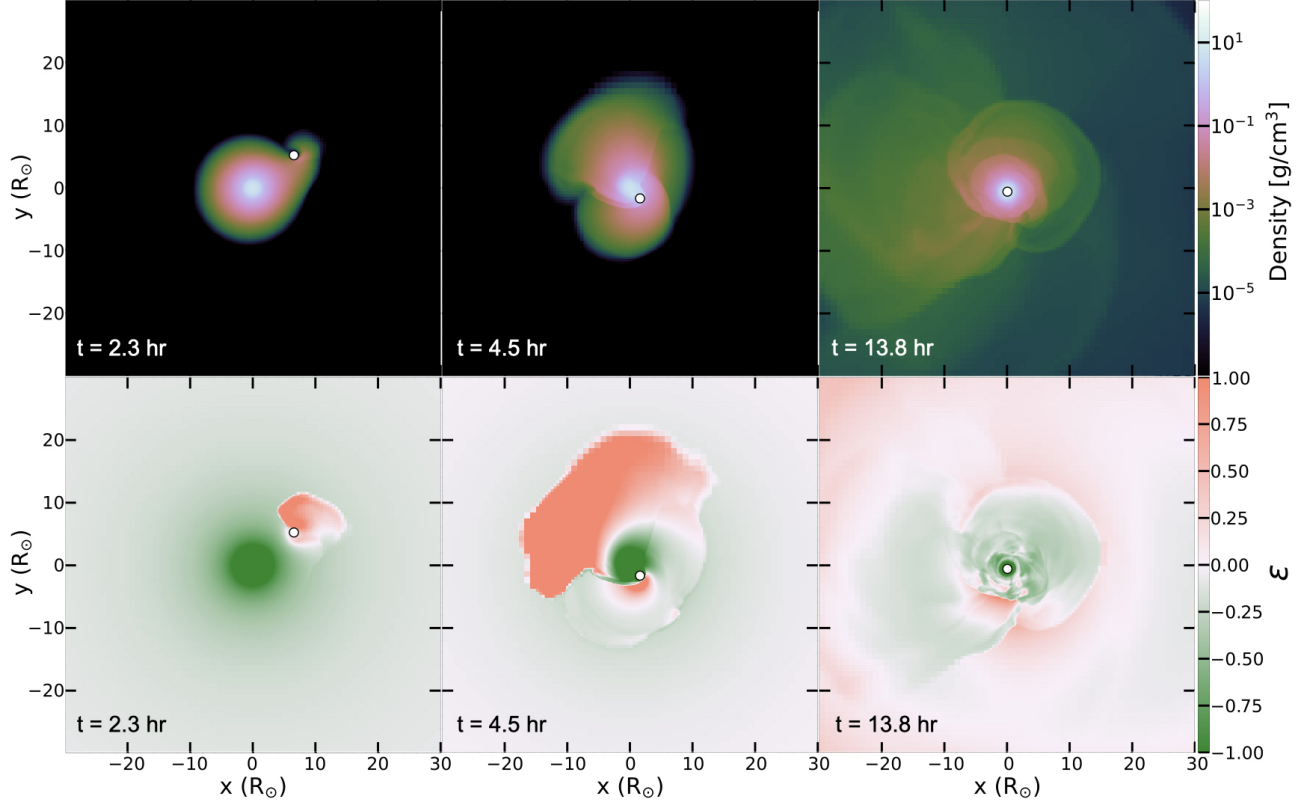


Figure 2. Two-dimensional slices across the orbital plane of FLASH simulated inspiral and merger of LMC X-4 at three stages: early in the evolution (2.3 hr), at an intermediate time when the NS enters the stellar core (4.5 hr), and at a late time (13.8 hr) when the NS has just reached the center of the stellar core. *Top panels:* Logarithm of gas density. *Bottom panels:* Sum of specific kinetic and potential energy, $\varepsilon = \varepsilon_{\text{kin}} + \varepsilon_{\text{grav}}$, in units of $10^{16} \text{ cm}^2/\text{s}^2$. The coral region corresponds to unbound material ($\varepsilon > 0$) and the green region corresponds to bound material ($\varepsilon < 0$).

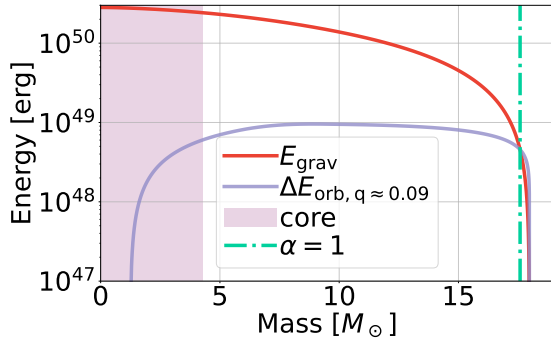


Figure 3. Relevant quantities required to estimate envelope unbinding during the merger, which are shown in mass coordinates. The binding energy of the primary's stellar material exterior to a given mass coordinate (E_{grav} , red line) and the change in orbital energy expected to be dissipated during the inspiral (ΔE_{orb} , $q \approx 0.09$, purple line) are plotted against the mass coordinate for the model used as the initial condition for hydrodynamical simulation, with mass $18 M_{\odot}$ and neutron star mass ratio $q \approx 0.09$. The mass coordinate at which the $\alpha = (E_{\text{grav}}/\Delta E_{\text{orb}}) = 1$ condition is satisfied is shown as a vertical dashed line.

$\approx 0.4 M_{\odot}$ of envelope material. Note that although this calculation is only approximate it allows us to better understand the results of a detailed simulation able to capture the energy sharing during the inspiral process.

Since the orbital energy deposited by the NS through inspiral is less than the gravitational binding energy of the stellar envelope, a merger is an inevitable outcome for LMC X-4. As the NS inspirals, the structure of the envelope internal to the position of the NS will remain fairly unaltered and the orbit of the NS will shrink until it merges with the stellar core.

We first note that the change in orbital energy continues to slightly increase although it remains well below the envelope's binding energy for the region between the core and the $\alpha = 1$ crossing point. As seen in Figure 2, the envelope is shocked and swept preferentially outwards as the NS moves through the envelope of the primary. Basically, the NS acts as a local diffusive energy source term, giving surrounding material roughly outward radial velocities. By the time the engulfed NS reaches the outer edge of the stellar core we find $\approx 1.4 M_{\odot}$ of mass to be unbound in our simulation (Figure 4) by summing the mass of the cells with $\varepsilon > 0$ at the $t = 4.5$ hr snapshot of our hydrodynamic simulation. This time is chosen as the moment when the NS reaches the core, and no envelope material has yet been ejected from the

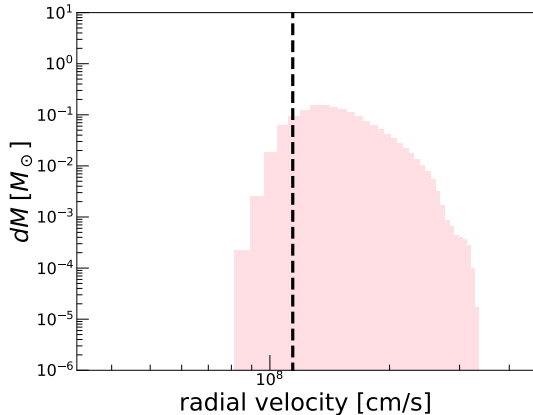


Figure 4. The outward radial velocity histogram of the debris expelled during the merger. This is done by analysing the velocity vectors and masses of each grid cell in the envelope with $\varepsilon > 0$ at $t = 4.5$ hr. The total mass ejected in the simulation during the merger is $\approx 1.4M_{\odot}$. Also plotted is the local escape velocity at the $\alpha = 1$ critical radius, which is computed based on the enclosed mass of the initial model (Figure 3). This velocity is $v_{\alpha=1} \approx 1140$ km/s and is shown as a vertical dashed line.

computational domain. The velocity vectors of each grid cell that meets this criterion at $t = 4.5$ hr are nearly all pointed radially outwards. The outward radial velocity distribution of the envelope material expelled during the merger episode is shown in Figure 4. The distribution shown in Figure 4 is compared to the local escape velocity at the $\alpha = 1$ critical radius, $v_{\alpha=1} \approx 1140$ km/s, which is computed based on the enclosed mass of the initial model (Figure 3). The deposited energy is not shared efficiently throughout the envelope (MacLeod et al. 2022) as the orbit of the NS shrinks and, as a result, shocks accelerate a non-negligible fraction of the envelope mass to well above the escape velocity.

We conclude that the $\alpha = 1$ condition provides a lower limit to the amount of energy injected into the stellar envelope. Some of the excess energy resides in the thermal energy content stored in the primary star (Fragos et al. 2019), which as the envelope expands, does work. In addition, as the NS continues to sink below the $\alpha = 1$ critical radius, a larger fraction of orbital energy can be injected into the envelope (Wu et al. 2020). As such, we must consider the internal energy (e.g., Fragos et al. 2019), the remaining orbital energy as the NS continues to sink (e.g., Wu et al. 2020; Law-Smith et al. 2020b) and the anisotropic sharing of this energy in the envelope (e.g., MacLeod et al. 2018) in order to better estimate the properties of the outflow. The outcomes of this study have direct consequences for the efficiency of envelope ejection, which is directly relevant to astronomical transients powered by recombination (e.g., MacLeod et al. 2017b; Schröder et al. 2020).

3.4. On the Accretion-fed Growth of the Neutron Star during the Merger Phase

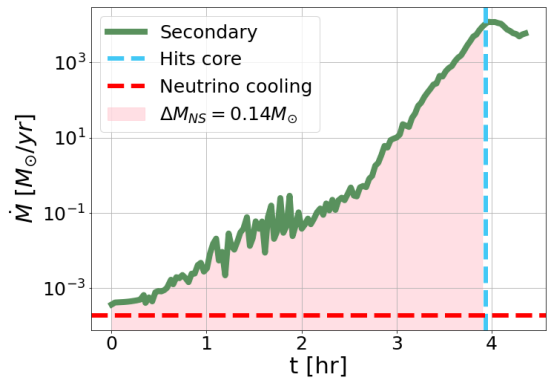


Figure 5. Mass accretion rate onto the inspiraling NS as a function of time during the simulation shown in Figure 2. In compact primaries, the NS is able to accrete above the limit at which neutrinos are able to provide the main cooling agent (red dashed line). In LMC X-4 the NS is able to gain about $0.14M_{\odot}$, but remains well below the maximum NS mass until merging with the core (blue dashed line).

The accretion-fed growth of NSs during CE events has been discussed extensively in the context of successful CE ejection. In these cases, possible outcomes include close binaries comprised of a He-star and a NS, which might leave behind a double NS or NS–BH binary (Postnov & Yungelson 2014). Accretion onto the NS during this phase was thought to be effectual as neutrinos provide a cooling mechanism (Houck & Chevalier 1991; Chevalier 1993; Fryer et al. 1996), suggesting that a NS might undergo accretion-induced collapse to a BH in some, but not all, cases (Chevalier 1993; Brown 1995; Bethe & Brown 1998).

The idea that a NS might be able to grow via accretion during CE is hard to reconcile with the observed distribution of NS masses (e.g., Özel et al. 2012) and, most notably, with those inferred in double NS binaries. These systems show a narrow range of inferred masses centered at $1.33M_{\odot}$ with dispersion of $0.05M_{\odot}$ (Özel et al. 2012). MacLeod & Ramirez-Ruiz (2015b) demonstrated that the presence of a density gradient in stellar envelopes significantly restricts accretion by imposing a net angular momentum to the flow around the NS, and that embedded NSs should accrete only modest amounts of envelope material. This study presented a clear hydrodynamical solution that successfully explains the narrow mass distribution seen in double NS binaries. This was later confirmed by Law-Smith et al. (2020b) with the use of global hydrodynamical simulations. These studies have been, however, restricted to survival of NSs in successful CE events. Further work is needed to probe the efficiency of accretion in NSs that are unable to eject the envelope and, as a result, merge with the dense core.

We now extend these calculations to consider the accretion history of the NS in LMC X-4. In Figure 5 we plot the mass accretion rate onto the inspiraling NS before reaching the core (dashed vertical line). We find that the NS is able to gain about $0.14M_{\odot}$ and the inferred accretion rate

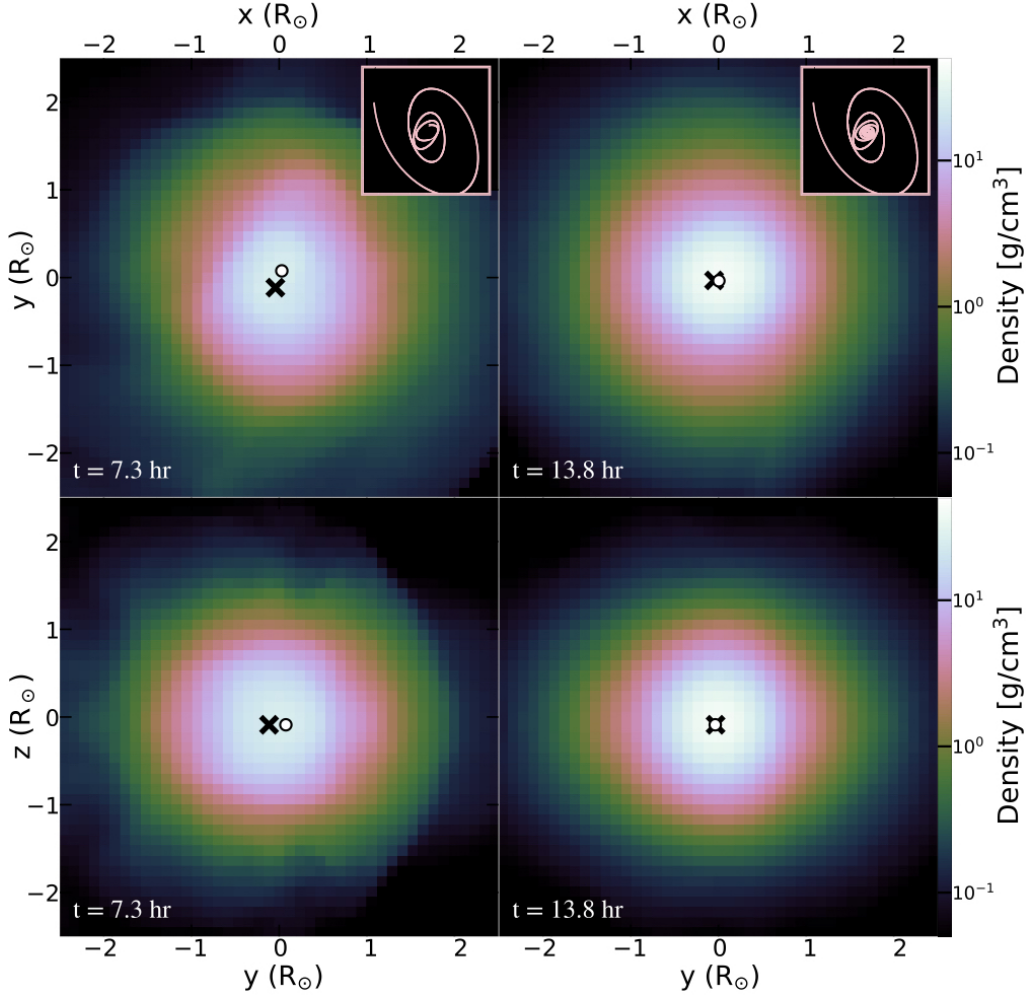


Figure 6. Two dimensional slices of the logarithm of gas density at two different times (7.3hr and 13.8hr) for material near the core of the primary. The *top* panels show slices in the orbital plane (y - x) while the *bottom* panels display slices in the vertical plane (y - z). The position of the core’s center of mass is denoted by an X mark, while the position of the NS is denoted by a white circle. The evolution of the trajectory of the NS in the orbital plane from the time the NS reaches the core is shown in the respective inset panels with a characteristic height and width of $(4R_\odot)^2$.

across the point mass remains above the neutrino-cooling rate, $\dot{M}_\nu \approx 10^4 \dot{M}_{\text{Edd}} \approx 10^{-4} M_\odot/\text{yr}$ (Houck & Chevalier 1991) at which accretion growth can proceed effectively. The results presented in Figure 5 are in agreement with the mass accretion rates derived using the formalism of MacLeod & Ramirez-Ruiz (2015b) for this specific progenitor. A limitation of most numerical models is that the accretion rate depends sensitively on the size of the central absorbing sink (e.g., Murguia-Berthier et al. 2017a; De et al. 2020), which implies that the results presented in Figure 5 are upper limits. This mass gain, nonetheless, represents a small fractional amount and won’t drastically affect the structure of the NS, which will remain well under the maximum mass limit.

3.5. Embedded Phase and Merger with the Stellar Core

Here, we take a closer look at the final plunge of the NS and its impact on core structure and final merger. Figure 6 provides a zoomed-in view of the stellar core near the end

of the inspiral. The relevant quantity fixing the strength of the interaction is $q_c^{1/3} = (M_{\text{NS}}/M_{\text{core}})^{1/3}$ (Everson et al. 2023) and, as such, we expect the NS to only mildly impact the stellar core. This is because $q_c < 1$, making the extent of the core larger than the tidal radius with respect to the NS (Everson et al. 2023). Shown in Figure 6 are illustrations of the gas density of the primary’s core at two different times, where the *top* panels show slices in the orbital plane (y - x), and the *bottom* panels display slices in the vertical plane (y - z). The two inset panels in Figure 6 show the trajectory of the NS in the orbital plane from the moment it reaches the core until the end of the simulation.

The core of the primary spins up due to shocks generated during inspiral, absorbing orbital angular momentum deposited by the NS. If the spin of the core material is lower than that required to form a disk, we can assume quasi-spherical accretion, which is necessary to power a classical TZO (Everson et al. 2023). If, on the other hand, the spin of

the core is higher than that required to form a disk, significant post-merger accretion feedback is expected to unbind the vast majority of the remaining envelope (Bavera et al. 2020; Murguia-Berthier et al. 2020). The post-merger angular momentum content of the stellar core is thus essential to defining the type of merger product that will result. Motivated by this, our aim in the next section is to discuss the post-merger flow pattern around the NS, involving accretion, rotation, and directional outflow.

4. IMPLICATIONS FOR THORNE-ŻYTKOW OBJECT FORMATION AND ULTRA-LONG GAMMA-RAY BURSTS

We now explore the final outcome of LMC X-4 as informed by our simulations. As a result of the merger, the NS injects energy, mass, and angular momentum into the core of the primary star (Figure 2) and unbinds a small amount of envelope material in the process (Figure 4). Shocks in the course of the inspiral spin up the core before the NS ultimately settles into the core’s interior (Figure 6). LMC X-4 thus naturally evolves into a collapsar-like progenitor system (Fryer & Woosley 1998). That is, a hyper-accreting NS surrounded by a rotating stellar core.

4.1. A Rapidly Rotating Stellar Core Accreting onto a Central Neutron Star

The first task in attempting to construct a general scheme that is able to successfully describe the fates of X-ray binaries such as LMC X-4 is to decide which parameters exert a controlling influence upon their final properties. The mass of the central object is a key parameter, as it dictates a characteristic luminosity scale for the ensuing accretion activity (e.g., Fryer & Woosley 1998) as well as determining the post-merger properties of the stellar core (Everson et al. 2023). The total angular momentum of the core may be, however, more important in this regard as it determines whether or not an accretion disk will be formed immediately upon merger.

Figure 7 displays the specific angular momentum content in the stellar core, calculated by taking the spherical average about the center of mass of the FLASH simulation shown in Figure 6. The specific angular momentum is shown in units of j_{iseco} (Bardeen et al. 1972), the minimum specific angular momentum required for disk formation, and is plotted against the enclosed mass, which includes the NS. As expected, the specific angular momentum is above the critical limits $j/j_{\text{iseco}}=1$ at all mass coordinates. We expect a BH to be formed when the NS reaches a mass of about $3M_{\odot}$ (pink shaded region in Figure 6). After the inevitable accretion-induced collapse of the NS, the expected outcome would then be a spinning BH surrounded by an accretion disk, which is reminiscent central engine models for gamma-ray burst (GRB) sources (Woosley 1993; Fryer & Woosley 1998; Mochkovitch et al. 1993; Rees 1999; MacFadyen & Woosley 1999; Aloy et al. 2000; Fryer & Heger 2000; MacFadyen et al. 2001; Lee & Ramirez-Ruiz 2007; Gehrels et al. 2009; Gottlieb et al. 2022).

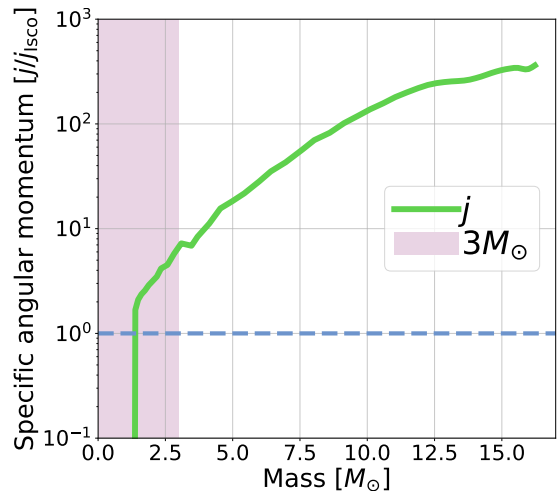


Figure 7. The normalized specific angular momentum content j/j_{iseco} of the stellar core at the end of the simulation is shown in mass coordinates (green curve). The profile is calculated by taking the spherical average about the center of mass in the FLASH simulation shown in Figure 6. Here j_{iseco} is the specific angular momentum required for disk formation about the NS; the simulated stellar model satisfies this condition for disk formation at all radii.

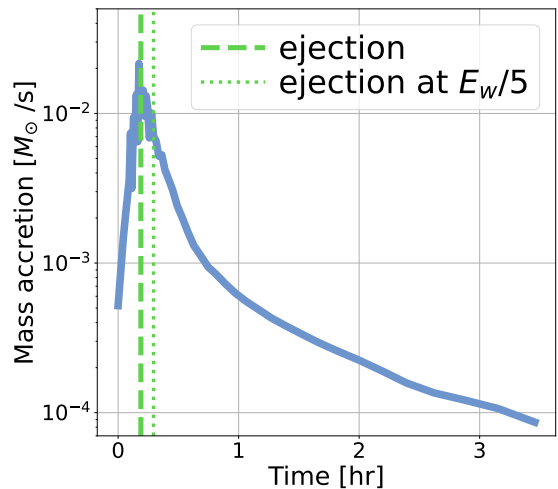


Figure 8. The accretion rate onto the newly formed BH as a function of time. The rotating in-falling core material is assumed to free fall without any pressure support and without mixing of radial layers. A disk is presumed to form from the collapse of every infalling shell and then subsequently accreted before the next shell collapses, as described in Bavera et al. (2020). When feedback from the accretion disk is taken into account, we show that it can unbind the infalling material on timescales that are comparable to the peak accretion time. The two ejection timescales shown as vertical lines are introduced in Figure 9.

To calculate the accretion rate history of the accreting BH we follow the framework described in [Batta & Ramirez-Ruiz \(2019\)](#) and [Bavera et al. \(2020\)](#). Following the assumption that a BH is formed from the collapse of the innermost $3M_{\odot}$ of the stellar core, we presume that the rotating in-falling material free falls onto the recently formed BH without any pressure support and without mixing of radial layers. In this formalism the mass distribution $M(r)$ of the stellar core can be envisioned as a collection of shells with mass m_{shell} and angular frequency Ω_{shell} that fall one after the other. Assuming that the disk formed from the collapse of a shell (m_{shell} with $j > j_{\text{isco}}$) is accreted before the next shell collapses, as the viscous accretion timescale of the inner disk is shorter than the dynamical timescale of the collapsing shells, we can calculate the accretion rate onto the BH, while consistently evolving the BH's mass and spin as material is amassed. The reader is referred to [Bavera et al. \(2020\)](#) for further details.

The resulting mass accretion rate is displayed in Figure 8. The peak accretion luminosity is, as expected, well below that expected for most collapsar models ($\gtrsim 10^{-1}M_{\odot}/\text{s}$; [Fryer & Woosley 1998](#); [MacFadyen & Woosley 1999](#)) and the central engine is foreseen to be longer lived than the typical duration of long GRBs ($\approx 20\text{ s}$; [Gehrels et al. 2009](#)). This is expected as the core of the primary star is not highly evolved and thus remains much less compact at the time of collapse.

The accretion activity might be, however, shortened when the feedback energy from the wind's accretion luminosity is taken into consideration. It has been widely shown that general relativistic, magnetohydrodynamic simulations of accretion disks around rotating BHs (e.g., [McKinney et al. 2012](#)) commonly show the development of a magnetized wind outflow, which can introduce energy that can, in this case, be competently shared with the layers of the infalling core. Figure 9 shows how the accumulated energy injection from the wind may contribute to envelope ejection as the stellar material infalls and subsequently accretes. The feedback from accretion is assumed to launch a wind that shares energy E_w with the collapsing stellar material with an efficiency of 1% (0.2%). The envelope is expected to be ejected when the integrated energy from the wind is larger than the binding energy of the envelope (see the dashed lines in Figure 9). This provides us with a rough idea of the total energy available to unbind the star. The feedback energy from accretion would then stop the collapse and notably abbreviate the duration of the accretion event.

4.2. Ultra-long GRBs and Recombination Transients

In this section we present a short summary of what we have learned so far about the fate of LMC X-4. Figure 10 presents a schematic montage of the events in the life of the LMC X-4 system. This encourages us to present a preliminary account of the effects of the ensuing accretion activity onto the central compact object. We also briefly describe the observational prospects for the near future. The NS at the center of the merger remnant quickly accretes a sizable amount of mass and is expected to collapse to a BH. The expected outcome

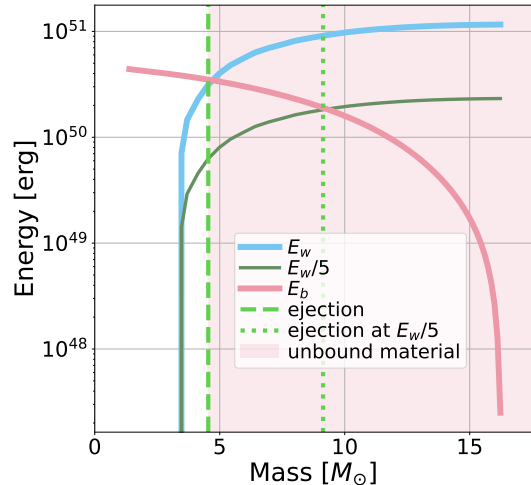


Figure 9. Relevant energy scales needed to estimate envelope unbinding during the accretion phase onto the newly formed BH. The binding energy of the rotating collapsing envelope, E_b , exterior to a given mass coordinate (pink) and the integrated wind accretion energy, E_w , expected to be shared with the infalling envelope (blue and dark green) are plotted against the mass coordinate of the post-merger model. The integrated energy required for ejection is uncertain. Here we assume two feedback efficiencies when calculating the fraction of energy that is shared with the collapsing stellar material. These are 1% (blue) and 0.2% (dark green), respectively. The formation of an accretion disk induces feedback, which in turn imposes a limit to the fraction of the star that can collapse and power an accretion event (dashed and dotted vertical lines).

would then be a spinning BH, orbited by a torus of stellar core debris. The binding energy of the orbiting debris and the spin of the BH are the two main energy reservoirs. It has become increasingly conspicuous that most plausible GRB progenitors (e.g., [Izzard et al. 2004](#); [Lee & Ramirez-Ruiz 2007](#); [Rees 1999](#); [Gehrels et al. 2009](#); [Murguía-Berthier et al. 2017b](#)) are expected to lead to a BH plus debris torus system with the overall energetics mainly determined by the mass and spin of the BH and the different masses left behind in the orbiting debris. This accretion process is expected to power and launch a relativistic jet, which will pierce through the primary star (e.g., [MacFadyen et al. 2001](#); [Ramirez-Ruiz et al. 2002](#); [Gottlieb et al. 2022](#)). Energy dissipation within the jet is expected to produce γ -ray emission, which will eventually be detected as a GRB for on-axis observers.

The expected properties, including luminosities and decay timescales, are consistent with properties of ultra-long GRBs (ULGRBs; e.g., [Levan et al. 2014](#)). These ULGRBs attain peak X-ray luminosities of $\approx 10^{49}\text{ erg/s}$, have a duration on the order of a few hours, and have non-thermal spectra evocative of relativistically beamed emission. In Figure 11, we plot the peak timescale and luminosity of the high energy transient following the merger of LMC X-4. We calculate the beamed luminosity of the jetted transient by assuming it traces the mass supply onto the BH, $L \propto \dot{M}c^2$ (Figure 8).

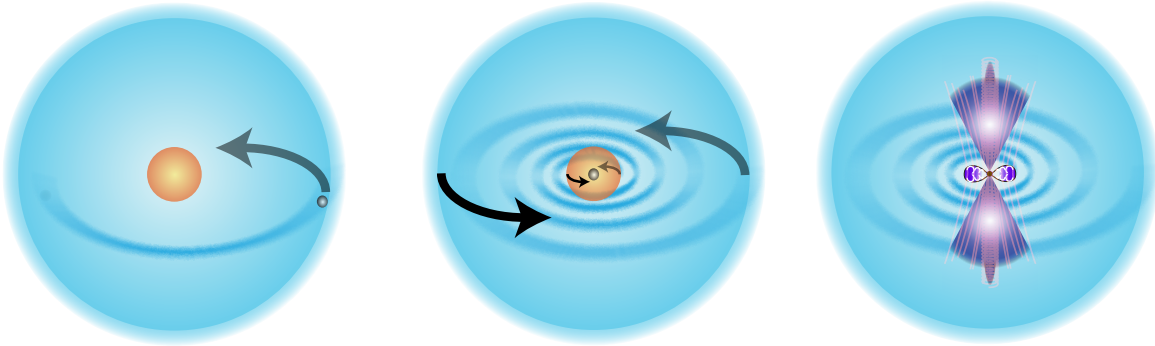


Figure 10. Diagram illustrating the post-merger evolution of the LMC X-4 system. After the primary fills its Roche lobe (represented by the blue sphere) and engulfs the NS (represented by the grey sphere), a merger event cannot be avoided (Figure 1). As the engulfment proceeds (Figure 6), the NS rapidly (≈ 13.8 hr) sinks into the core (represented by the orange sphere). As a result, the core spins up due to shocks produced in the course of the inspiral. The further evolution of the rapidly rotating merger product can produce several interesting phenomena. The neutron star is expected to accrete a significant amount of mass to collapse to a BH. The rotating core, as it continues to collapse, will produce an accretion disk (Figure 7), which will likely also power and launch a relativistic jet.

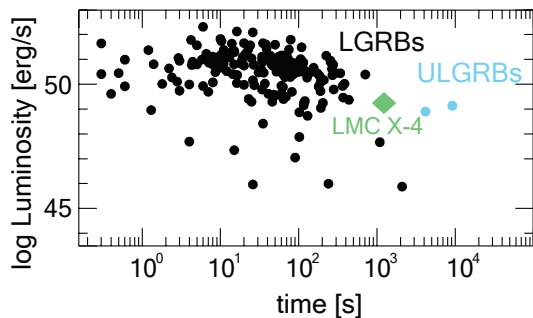


Figure 11. Luminosity as a function of the duration of high-energy transients adapted from [Levan et al. \(2014\)](#). For the GRB and ULGRB sources we plot t_{90} as the duration and the peak isotropic luminosity. The duration of the event assumes the *ejection* timescale determined by accretion feedback in Figure 8. The properties of the high-energy transient roughly coincide with those of the emerging class of ultra-long GRBs, such as GRB 101225A, GRB 111209A, and GRB 121027A.

We also assume that 1% of the accretion luminosity goes into high-energy radiation. It is thus enticing to identify ultra-long GRBs with the catastrophic merger of a compact object with a primary star with a small fraction of accretion energy going into a jetted outflow. This could be the less extreme example of a collapsar progenitor ([Woosley 1993](#); [MacFadyen & Woosley 1999](#)).

If we were to venture a general classification scheme for the fate of HMXBs, on the hypothesis that the central engine involves a BH formed in the collapse of post-merger stellar cores ([Everson et al. 2023](#)), we would surely expect the mass of the BH, the rate at which the gas is supplied to the BH (which will depend on the mass and evolutionary state of the primary star), the spin of the BH, and the orientation relative to our line of sight to all be essential parameters. For off-axis observers, we expect the mass ejected from the

merger and the ensuing feedback to power an optical or infrared transient as it expands and becomes transparent ([Soker & Tylenda 2006](#); [Metzger et al. 2012](#); [Ivanova et al. 2013](#); [MacLeod et al. 2017b](#)). The detection of this post-merger transient would offer direct constraints on the properties of the outflow such as the total mass and velocity distribution. We expect that the ensuing accretion feedback, which will likely halt accretion, would help unbind most of the stellar envelope and thus produce a much brighter recombination transient than the one expected from the outflow conditions shown in Figure 4.

4.3. Thin-envelope TZOs

After nearly all of the stellar envelope has been unbound and ejected by the nascent BH, for systems with compact primaries such as LMC X-4, an alternative type of steady-state merger product may be possible: the thin-envelope TZO (TETZO) as proposed by [Everson et al. \(2023\)](#). The TETZO is comprised of a central BH accreting via disk surrounded by a diffuse, radiation supported, remnant envelope with $\lesssim 1\%$ of the envelope’s initial mass, that is powered by the BH’s accretion luminosity. The TETZO is not unlike the classical TZO, though rather than presenting similarly to a star in the optical bands, these would present as ultra-luminous X-ray sources with a lifetime of $\approx 10^4$ yrs ([Everson et al. 2023](#)).

Thus, the fate of LMC X-4 is unlikely to lead to a configuration as a TZO due to the effects of rotation as described above, but if any envelope remains after the series of transient events initiated by the merger, this and other close HMXBs may end their lives as something not altogether different from what Thorne & Żytkow envisioned nearly 50 years ago.

5. SUMMARY

In this paper we investigate the long-term fate of high mass X-ray binaries with the objective of understanding whether a TZO might be ultimately assembled. We present the results from a start-to-end 3D hydrodynamical simulation aimed at studying the fate of LMC X-4, a tight high mass X-ray binary

system, after the primary star fills its Roche lobe and engulfs the NS companion (Figure 10). The salient findings of this work are:

- The NS, as a consequence of the merger, injects energy, mass, and angular momentum into the core of the primary star (Figure 2). Spiral shocks during the merger spin up the core of the primary star before the NS eventually settles into the core’s interior (Figure 6). LMC X-4 thus plainly develops into a hyper-accreting NS surrounded by a rotating stellar core, similar to a collapsar-like progenitor system (Figure 7).
- The inspiraling NS, upon merging with the core, can accrete efficiently at high rates (Figure 8), subsequently collapsing into a BH. This accretion process is expected to power and launch a relativistic jet, which will pierce through the envelope of the primary star and trigger a bright transient with a luminosity and duration typical of an ultra-long GRB (Figure 11). Such high-energy transients can be uncovered by observers along the jet axis.
- Significant post-merger accretion feedback will unavoidably unbind the vast majority of the surrounding envelope, powering an optical or infrared transient as the material expands, recombines and becomes transparent. The detection of this transient, which will be available to observers at all directions, would offer direct constraints on the conditions and flow properties of this highly uncertain phase of high-mass X-ray binary evolution.
- After most of the stellar envelope is ejected by the newly formed BH, we expect a thin-envelope TZO to form, as predicted by [Everson et al. \(2023\)](#). This short-lived source ($\approx 10^4$ yrs) will manifest as an ultra-luminous X-ray source. As such, the canonical frame-

work for TZO formation via common envelope evolution needs to be revisited. This is due to the fact that the post-merger angular momentum content of the material is, for all merging binaries ([Everson et al. 2023](#)), high enough to break spherical symmetry and produce a centrifugally supported accretion disk.

We gratefully acknowledge S. Wu, A. Mannings, A. Hermosillo Ruiz, M. MacLeod, A. Vigna-Gómez, R. Foley, D. Coulter, and S. Schröder for helpful discussions. R.W.E. acknowledges the support of the University of California President’s Dissertation-Year and Eugene V. Cota-Robles Fellowships, the Heising-Simons Foundation, the ARCS Foundation, and the Vera Rubin Presidential Chair at UCSC. This material is based upon work supported by the National Science Foundation Graduate Research Fellowship Program under Grant No. 1339067. RY is grateful for support from a Doctoral Fellowship from the University of California Institute for Mexico and the United States (UCMEXUS), a Texas Advanced Computing Center (TACC) Frontera Computational Science Fellowship, and a NASA FINESST award (21-ASTRO21-0068). E.R.-R. acknowledges support from the Heising-Simons Foundation and the National Science Foundation (2150255 and 2307710). Any opinions, findings, and conclusions or recommendations expressed in this material are those of the authors and do not necessarily reflect the views of the NSF. The 3D hydrodynamics software used in this work was developed in part by the DOE NNSA- and DOE Office of Science-supported Flash Center for Computational Science at the University of Chicago and the University of Rochester.

Software: FLASH ([Fryxell et al. 2000](#)), Python, MESA ([Paxton et al. 2011, 2013, 2015, 2018, 2019](#)), matplotlib ([Hunter 2007](#)), yt ([Turk et al. 2011](#)), NumPy ([van der Walt et al. 2011](#)), py_mesa_reader ([Wolf & Schwab 2017](#))

REFERENCES

- Aloy, M. A., Müller, E., Ibáñez, J. M., Martí, J. M., & MacFadyen, A. 2000, *ApJL*, 531, L119, doi: [10.1086/312537](#)
- Bardeen, J. M., Press, W. H., & Teukolsky, S. A. 1972, *ApJ*, 178, 347, doi: [10.1086/151796](#)
- Batta, A., & Ramirez-Ruiz, E. 2019, arXiv e-prints, arXiv:1904.04835, doi: [10.48550/arXiv.1904.04835](#)
- Bavera, S. S., Fragos, T., Qin, Y., et al. 2020, *A&A*, 635, A97, doi: [10.1051/0004-6361/201936204](#)
- Beasar, E. R., Davies, B., Cabrera-Ziri, I., & Hurst, G. 2018, *MNRAS*, 479, 3101, doi: [10.1093/mnras/sty1744](#)
- Belczynski, K., Kalogera, V., & Bulik, T. 2002, *ApJ*, 572, 407, doi: [10.1086/340304](#)
- Bethe, H. A., & Brown, G. E. 1998, *ApJ*, 506, 780, doi: [10.1086/306265](#)
- Biehle, G. T. 1991, *ApJ*, 380, 167, doi: [10.1086/170572](#)
- Brown, G. E. 1995, *ApJ*, 440, 270, doi: [10.1086/175268](#)
- Cannon, R. C., Eggleton, P. P., Zytzkow, A. N., & Podsiadlowski, P. 1992, *ApJ*, 386, 206, doi: [10.1086/171006](#)
- Chernov, S. 2020, *Astronomy Reports*, 64, 425, doi: [10.1134/S1063772920050017](#)
- Chevalier, R. A. 1993, *ApJL*, 411, L33, doi: [10.1086/186905](#)
- Choi, J., Dotter, A., Conroy, C., et al. 2016, *ApJ*, 823, 102
- Choudhury, S., de Grijs, R., Bekki, K., et al. 2021, *MNRAS*, 507, 4752
- De, S., MacLeod, M., Everson, R. W., et al. 2020, *ApJ*, 897, 130, doi: [10.3847/1538-4357/ab9ac6](#)
- Dotter, A. 2016, *ApJS*, 222, 8
- Everson, R. W., Hutchinson-Smith, T., Vigna-Gómez, A., & Ramirez-Ruiz, E. 2023, arXiv e-prints, arXiv:2310.08658, doi: [10.48550/arXiv.2310.08658](#)

- Everson, R. W., MacLeod, M., De, S., Macias, P., & Ramirez-Ruiz, E. 2020, *ApJ*, 899, 77, doi: [10.3847/1538-4357/aba75c](https://doi.org/10.3847/1538-4357/aba75c)
- Falanga, M., Bozzo, E., Lutovinov, A., et al. 2015, *A&A*, 577, A130, doi: [10.1051/0004-6361/201425191](https://doi.org/10.1051/0004-6361/201425191)
- Falanga, M., Bozzo, E., Lutovinov, A., et al. 2015, *A&A*, 577, 130, doi: [10.1051/0004-6361/201425191](https://doi.org/10.1051/0004-6361/201425191)
- Farmer, R., Renzo, M., Göteborg, Y., et al. 2023, *MNRAS*, 524, 1692, doi: [10.1093/mnras/stad1977](https://doi.org/10.1093/mnras/stad1977)
- Fragos, T., Andrews, J. J., Ramirez-Ruiz, E., et al. 2019, *ApJL*, 883, L45, doi: [10.3847/2041-8213/ab40d1](https://doi.org/10.3847/2041-8213/ab40d1)
- Fryer, C. L., Benz, W., & Herant, M. 1996, *ApJ*, 460, 801, doi: [10.1086/177011](https://doi.org/10.1086/177011)
- Fryer, C. L., & Heger, A. 2000, *ApJ*, 541, 1033, doi: [10.1086/309446](https://doi.org/10.1086/309446)
- Fryer, C. L., & Woosley, S. E. 1998, *ApJL*, 502, L9, doi: [10.1086/311493](https://doi.org/10.1086/311493)
- Fryxell, B., Olson, K., Ricker, P., et al. 2000, *ApJS*, 131, 273, doi: [10.1086/317361](https://doi.org/10.1086/317361)
- Gallegos-Garcia, M., Fishbach, M., Kalogera, V., L Berry, C. P., & Doctor, Z. 2022, *ApJL*, 938, L19, doi: [10.3847/2041-8213/ac96ef](https://doi.org/10.3847/2041-8213/ac96ef)
- Gehrels, N., Ramirez-Ruiz, E., & Fox, D. B. 2009, *ARA&A*, 47, 567, doi: [10.1146/annurev.astro.46.060407.145147](https://doi.org/10.1146/annurev.astro.46.060407.145147)
- Gottlieb, O., Lalakos, A., Bromberg, O., Liska, M., & Tchekhovskoy, A. 2022, *MNRAS*, 510, 4962, doi: [10.1093/mnras/stab3784](https://doi.org/10.1093/mnras/stab3784)
- Guillochon, J., & Ramirez-Ruiz, E. 2013, *ApJ*, 767, 25, doi: [10.1088/0004-637X/767/1/25](https://doi.org/10.1088/0004-637X/767/1/25)
- Guillochon, J., Ramirez-Ruiz, E., Rosswog, S., & Kasen, D. 2009, *ApJ*, 705, 844, doi: [10.1088/0004-637X/705/1/844](https://doi.org/10.1088/0004-637X/705/1/844)
- Halevi, G., Wu, B., Mösta, P., et al. 2023, *ApJL*, 944, L38, doi: [10.3847/2041-8213/acb702](https://doi.org/10.3847/2041-8213/acb702)
- Houck, J. C., & Chevalier, R. A. 1991, *ApJ*, 376, 234, doi: [10.1086/170272](https://doi.org/10.1086/170272)
- Hoyle, F., & Lyttleton, R. A. 1939, *Proceedings of the Cambridge Philosophical Society*, 35, 405, doi: [10.1017/S0305004100021150](https://doi.org/10.1017/S0305004100021150)
- Hunter, J. D. 2007, *CSE*, 9, 90, doi: [10.1109/MCSE.2007.55](https://doi.org/10.1109/MCSE.2007.55)
- Ivanova, N., Justham, S., Avendano Nandez, J. L., & Lombardi, J. C. 2013, *Science*, 339, 433, doi: [10.1126/science.1225540](https://doi.org/10.1126/science.1225540)
- Izzard, R. G., Ramirez-Ruiz, E., & Tout, C. A. 2004, *MNRAS*, 348, 1215, doi: [10.1111/j.1365-2966.2004.07436.x](https://doi.org/10.1111/j.1365-2966.2004.07436.x)
- Law-Smith, J., Guillochon, J., & Ramirez-Ruiz, E. 2019, *ApJL*, 882, L25, doi: [10.3847/2041-8213/ab379a](https://doi.org/10.3847/2041-8213/ab379a)
- Law-Smith, J. A. P., Coulter, D. A., Guillochon, J., Mockler, B., & Ramirez-Ruiz, E. 2020a, *ApJ*, 905, 141, doi: [10.3847/1538-4357/abc489](https://doi.org/10.3847/1538-4357/abc489)
- Law-Smith, J. A. P., Everson, R. W., Ramirez-Ruiz, E., et al. 2020b, *arXiv e-prints*, arXiv:2011.06630, doi: [10.48550/arXiv.2011.06630](https://doi.org/10.48550/arXiv.2011.06630)
- Lee, W. H., & Ramirez-Ruiz, E. 2006, *ApJ*, 641, 961, doi: [10.1086/500533](https://doi.org/10.1086/500533)
- . 2007, *New Journal of Physics*, 9, 17, doi: [10.1088/1367-2630/9/1/017](https://doi.org/10.1088/1367-2630/9/1/017)
- Levan, A. J., Tanvir, N. R., Starling, R. L. C., et al. 2014, *ApJ*, 781, 13, doi: [10.1088/0004-637X/781/1/13](https://doi.org/10.1088/0004-637X/781/1/13)
- Levesque, E. M., Massey, P., Zytkow, A. N., & Morrell, N. 2014, *MNRAS*, 443, L94, doi: [10.1093/mnras/slu080](https://doi.org/10.1093/mnras/slu080)
- Levine, A. M., Rappaport, S. A., & Zojcheski, G. 2000, *ApJ*, 541, 194, doi: [10.1086/309398](https://doi.org/10.1086/309398)
- Liotine, C., Zevin, M., Berry, C. P. L., Doctor, Z., & Kalogera, V. 2023, *ApJ*, 946, 4, doi: [10.3847/1538-4357/acb8b2](https://doi.org/10.3847/1538-4357/acb8b2)
- Liu, Q. Z., van Paradijs, J., & van den Heuvel, E. P. J. 2006, *A&A*, 455, 1165, doi: [10.1051/0004-6361:20064987](https://doi.org/10.1051/0004-6361:20064987)
- Maccarone, T. J., & de Mink, S. E. 2016, *MNRAS*, 458, L1, doi: [10.1093/mnras/slww004](https://doi.org/10.1093/mnras/slww004)
- MacFadyen, A. I., & Woosley, S. E. 1999, *ApJ*, 524, 262, doi: [10.1086/307790](https://doi.org/10.1086/307790)
- MacFadyen, A. I., Woosley, S. E., & Heger, A. 2001, *ApJ*, 550, 410, doi: [10.1086/319698](https://doi.org/10.1086/319698)
- MacLeod, M., Antoni, A., Murguia-Berthier, A., Macias, P., & Ramirez-Ruiz, E. 2017a, *ApJ*, 838, 56, doi: [10.3847/1538-4357/aa6117](https://doi.org/10.3847/1538-4357/aa6117)
- MacLeod, M., De, K., & Loeb, A. 2022, *ApJ*, 937, 96, doi: [10.3847/1538-4357/ac8c31](https://doi.org/10.3847/1538-4357/ac8c31)
- MacLeod, M., Macias, P., Ramirez-Ruiz, E., et al. 2017b, *ApJ*, 835, 282, doi: [10.3847/1538-4357/835/2/282](https://doi.org/10.3847/1538-4357/835/2/282)
- MacLeod, M., Ostriker, E. C., & Stone, J. M. 2018, *ApJ*, 868, 136, doi: [10.3847/1538-4357/aae9eb](https://doi.org/10.3847/1538-4357/aae9eb)
- MacLeod, M., & Ramirez-Ruiz, E. 2015a, *ApJ*, 803, 41, doi: [10.1088/0004-637X/803/1/41](https://doi.org/10.1088/0004-637X/803/1/41)
- . 2015b, *ApJL*, 798, L19, doi: [10.1088/2041-8205/798/1/L19](https://doi.org/10.1088/2041-8205/798/1/L19)
- McKinney, J. C., Tchekhovskoy, A., & Blandford, R. D. 2012, *MNRAS*, 423, 3083, doi: [10.1111/j.1365-2966.2012.21074.x](https://doi.org/10.1111/j.1365-2966.2012.21074.x)
- Metzger, B. D., Giannios, D., & Spiegel, D. S. 2012, *MNRAS*, 425, 2778, doi: [10.1111/j.1365-2966.2012.21444.x](https://doi.org/10.1111/j.1365-2966.2012.21444.x)
- Mochkovitch, R., Hernanz, M., Isern, J., & Martin, X. 1993, *Nature*, 361, 236, doi: [10.1038/361236a0](https://doi.org/10.1038/361236a0)
- Murguia-Berthier, A., Batta, A., Janiuk, A., et al. 2020, *ApJL*, 901, L24, doi: [10.3847/2041-8213/abb818](https://doi.org/10.3847/2041-8213/abb818)
- Murguia-Berthier, A., MacLeod, M., Ramirez-Ruiz, E., Antoni, A., & Macias, P. 2017a, *ApJ*, 845, 173, doi: [10.3847/1538-4357/aa8140](https://doi.org/10.3847/1538-4357/aa8140)
- Murguia-Berthier, A., Ramirez-Ruiz, E., Montes, G., et al. 2017b, *ApJL*, 835, L34, doi: [10.3847/2041-8213/aa5b9e](https://doi.org/10.3847/2041-8213/aa5b9e)
- O'Grady, A. J. G., Drout, M. R., Shappee, B. J., et al. 2020, *ApJ*, 901, 135, doi: [10.3847/1538-4357/abafad](https://doi.org/10.3847/1538-4357/abafad)
- Özel, F., Psaltis, D., Narayan, R., & Santos Villarreal, A. 2012, *ApJ*, 757, 55, doi: [10.1088/0004-637X/757/1/55](https://doi.org/10.1088/0004-637X/757/1/55)

- Paczynski, B. 1976, in *Structure and Evolution of Close Binary Systems*, ed. P. Eggleton, S. Mitton, & J. Whelan, Vol. 73, 75
- Paxton, B., Bildsten, L., Dotter, A., et al. 2011, *ApJS*, 192, 3, doi: [10.1088/0067-0049/192/1/3](https://doi.org/10.1088/0067-0049/192/1/3)
- Paxton, B., Cantiello, M., Arras, P., et al. 2013, *ApJS*, 208, 4, doi: [10.1088/0067-0049/208/1/4](https://doi.org/10.1088/0067-0049/208/1/4)
- Paxton, B., Marchant, P., Schwab, J., et al. 2015, *ApJS*, 220, 15, doi: [10.1088/0067-0049/220/1/15](https://doi.org/10.1088/0067-0049/220/1/15)
- Paxton, B., Schwab, J., Bauer, E. B., et al. 2018, *ApJS*, 234, 34, doi: [10.3847/1538-4365/aaa5a8](https://doi.org/10.3847/1538-4365/aaa5a8)
- Paxton, B., Smolec, R., Schwab, J., et al. 2019, *ApJS*, 243, 10, doi: [10.3847/1538-4365/ab2241](https://doi.org/10.3847/1538-4365/ab2241)
- Postnov, K. A., & Yungelson, L. R. 2014, *Living Reviews in Relativity*, 17, 3, doi: [10.12942/lrr-2014-3](https://doi.org/10.12942/lrr-2014-3)
- Qin, Y., Marchant, P., Fragos, T., Meynet, G., & Kalogera, V. 2019, *ApJL*, 870, L18, doi: [10.3847/2041-8213/aaf97b](https://doi.org/10.3847/2041-8213/aaf97b)
- Ramirez-Ruiz, E., Celotti, A., & Rees, M. J. 2002, *MNRAS*, 337, 1349, doi: [10.1046/j.1365-8711.2002.05995.x](https://doi.org/10.1046/j.1365-8711.2002.05995.x)
- Rees, M. J. 1999, *A&AS*, 138, 491, doi: [10.1051/aas:1999324](https://doi.org/10.1051/aas:1999324)
- Safi-Harb, S., & Ögelman, H. 1996, *ApJ*, 456, L37
- Schröder, S. L., MacLeod, M., Loeb, A., Vigna-Gómez, A., & Mandel, I. 2020, *ApJ*, 892, 13, doi: [10.3847/1538-4357/ab7014](https://doi.org/10.3847/1538-4357/ab7014)
- Soker, N., & Tylenda, R. 2006, *MNRAS*, 373, 733, doi: [10.1111/j.1365-2966.2006.11056.x](https://doi.org/10.1111/j.1365-2966.2006.11056.x)
- Thorne, K. S., & Żytkow, A. N. 1975, *ApJL*, 199, L19, doi: [10.1086/181839](https://doi.org/10.1086/181839)
- . 1977, *ApJ*, 212, 832, doi: [10.1086/155109](https://doi.org/10.1086/155109)
- Timmes, F. X., & Swesty, F. D. 2000, *ApJS*, 126, 501, doi: [10.1086/313304](https://doi.org/10.1086/313304)
- Tout, C. A., Żytkow, A. N., Church, R. P., et al. 2014, *MNRAS*, 445, L36, doi: [10.1093/mnras/lu131](https://doi.org/10.1093/mnras/lu131)
- Turk, M. J., Smith, B. D., Oishi, J. S., et al. 2011, *ApJS*, 192, 9, doi: [10.1088/0067-0049/192/1/9](https://doi.org/10.1088/0067-0049/192/1/9)
- van den Heuvel, E. P. J. 1976, in *Structure and Evolution of Close Binary Systems*, ed. P. Eggleton, S. Mitton, & J. Whelan, Vol. 73, 35
- van der Walt, S., Colbert, S. C., & Varoquaux, G. 2011, *CSE*, 13, 22, doi: [10.1109/MCSE.2011.37](https://doi.org/10.1109/MCSE.2011.37)
- Wolf, B., & Schwab, J. 2017, *wmwwolf/py_mesa_reader: Interact with MESA Output*, Zenodo, doi: [10.5281/zenodo.826958](https://doi.org/10.5281/zenodo.826958)
- Woosley, S. E. 1993, *ApJ*, 405, 273, doi: [10.1086/172359](https://doi.org/10.1086/172359)
- Wu, S., Everson, R. W., Schneider, F. R. N., Podsiadlowski, P., & Ramirez-Ruiz, E. 2020, *ApJ*, 901, 44, doi: [10.3847/1538-4357/abaf48](https://doi.org/10.3847/1538-4357/abaf48)